

Influence of Welding Parameters on Macrostructure, Microstructure and Mechanical Properties in Orbital Pipe Welding of A36 Mild Steel Pipe

Ario Sunar Baskoro^{1*}, Gandjar Kiswanto¹, Agus Widianto¹, Muchamad Panji¹

¹Department of Mechanical Engineering, Faculty of Engineering,
Universitas Indonesia, Kampus Baru UI Depok, 16424, INDONESIA

*Corresponding Author

DOI: <https://doi.org/10.30880/ijie.2021.13.07.033>

Received 8 January 2021; Accepted 26 April 2021; Available online 30 September 2021

Abstract: In this work, the influence of welding parameters on macrostructure, microstructure and mechanical properties in Gas Tungsten Arc Welding (GTAW) orbital pipe welding was investigated. The aim of this study was to evaluate the effect of GTAW orbital pipe welding parameters on macrostructure, microstructure and tensile strength. This experiment using A36 mild steel pipe material with a thickness of 0.6 mm and an outer diameter of 114.3 mm. The joining method used is the V-groove joint without gaps with the ER70-S 6 wire feeder. Welding results were analyzed in macro and micro graphs, as well as analysis of tensile strength. Macro-graphic analyses revealed the depth of weld penetration that occurs as well as the boundaries of each welding area. The micro-graphic analysis shows structural changes that occur in the welding area. Welding parameters with a welding current of 170 A, a welding speed of 0.9 mm/s and a welding position of 0° have a Ultimate Tensile Strength (UTS) increase of 11.01% over the base metal. The highest and lowest UTS are 502.80 MPa and 280.77 MPa, respectively. The fracture surface in the weld area shows that many micro-voids and dimples were formed.

Keywords: Pipe welding, macrostructure, microstructure, A36 mild steel

1. Introduction

Pipe welding has an essential role in the oil, gas, and water industry. The piping system effectively means transporting oil, gas, and water from one place to another [1]. In piping systems, orbital pipe welding is usually used, where the pipe is at rest while the welding torch is rotating around the pipe [2]. Keeping the orbital pipe weld stable for all welding positions is one of the challenges of this welding.

One type of steel that is often used in piping systems is mild steel of A36. A36 mild steel has a lower price, widely available, and has a wider range of engineering applications. A36 mild steel is often used in many sectors such as construction, machine structures, ships, and bridges [3]. A36 mild steel is a material that is susceptible to corrosion if it is not treated after welding [4]. Surely this can be a problem if it is applied in a piping system to drain liquid.

Panji et al. [1] reported their research on the effect of welding parameters on the geometric characteristics and distortion of A36 mild steel. The results showed that the welding parameters impacted the amount of distortion at the close of the welding. Microstructure changes occur in mild steel A36 after being welded using Resistance Spot Welding (RSW), wherein the weld area there were many lath martensite and upper bainite structures [5]. Baskoro et al. [4] performed an optimization of the Gas Metal Arc Welding (GMAW) welding parameters to obtain minimal distortion on A36 mild steel, where optimization used the Taguchi and ANOVA methods. Liying et al. [6] evaluated their research on the effect of added material variations in the L415 / 316L material by the pipe welding method. It was found that the pitting holes in the ferric chloride solution indicated that the ER309MoL welding wire was not suitable

for welding the 316L layer. The Longitudinal Submerged Arc Welding (LSAW) method used to join C–Mn pipeline steel plates in a piping system was reported by Fan et al. [7]. The microstructure formed in the fine-grained and very fine weld area. Amuda et al. [8] reported the results mechanical properties with pre-weld thermal higher than with post-weld thermal, while the microstructure with pre-weld thermal exhibited coarse grain morphology in contrast to refined morphology in post thermally treated welds.

Several of the studies above show the results of research on pipe welding using A36 mild steel material. No studies analyze the macro structure, microstructure, and tensile strength of Gas Tungsten Arc Welding (GTAW) orbital pipe welding with A36 material. The purpose of this study was to evaluate the effect of GTAW orbital pipe welding parameters on macrostructure, microstructure, and tensile strength. A36 mild steel with a thickness of 6 mm is selected and is joined by the V-groove join and the ER70S-6 wire feeder. Macro-graphic and micro-graphic analyzes were applied to observe the effect of parameter variations. In addition, the analysis of the tensile strength and the location of the fracture is also done.

2. Methods and Material

A36 mild steel pipe with an outer diameter of 114.3 mm, length of 55 mm and thickness of 6 mm was used in this experiment. Wire feeder ER 70S-6 with a diameter of 1.6 mm was used to join the two specimens using the V-groove method without gaps [1]. The V-groove angle was 30 degrees for each specimen. Figure 1a shows the schematic illustration of the cross-section V-groove pipe join. Table 1 and Table 2 show the chemical composition of the A36 mild steel material and the ER-70S-6 wire feeder.

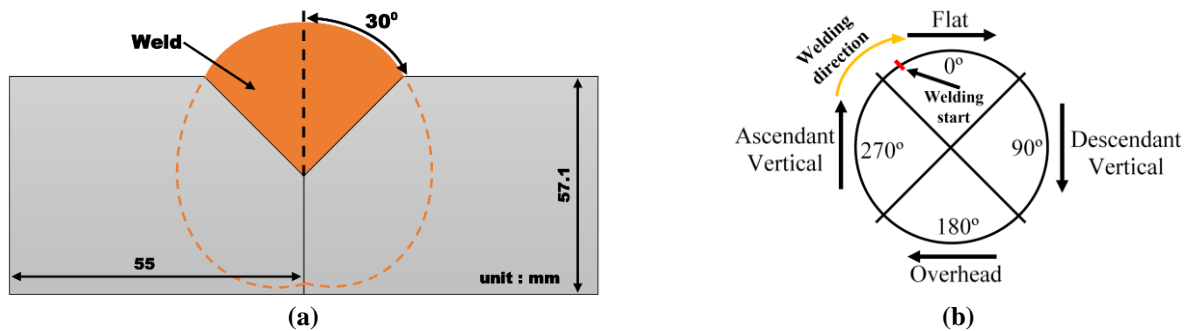


Fig. 1 - (a) Schematic illustration of cross-section V-groove pipe join; (b) Welding position in orbital pipe welding

Table 1 - Chemical composition (wt %) of A36 mild steel pipe [1]

A36	C	Si	Mn	P	S	Cr	Mo
	0.183	0.233	0.392	0.013	0.007	0.017	<0.005
	Ni	Al	Cu	Nb	Ti	V	Fe
<0.005	0.003	0.007	<0.002	<0.002	<0.002	<0.002	bal.

Table 2 - Chemical composition (wt %) of ER-70S 6 [1]

ER-70S 6	C	Si	P	S	Cu
	0.06	0.8	0.025	0.03	0.5

All specimens were sanded using sandpaper with a roughness of 240, 600 and 1000. Then to clean the remaining dirt using acetone solution. Dynasty 210 DX welding machine was used in this work with Gas Tungsten Arc Welding (GTAW) type welding. The argon gas flow rate used is 11 L/min to protect the outside of the welded pipe from oxidation. The electrode used was the EWTh-2 electrode with a red code and a sharpening angle of 25 degrees. The pipe is welded at the 5G position, and welding begins at a pipe angle of 330 degrees (see in Figure 1b) [1]. Table 3 shows the welding parameters of the orbital pipe.

Weld specimens were cut at four-pipe positions (0°, 90°, 180°, and 270°) for macrostructure and microstructure preparation. The specimen dimensions for macrostructure and microstructure observations are 20x30 mm. After being cut, the specimens are mounted using resin and allowed to stand until dry and hard. Then the specimen preparation was required for this process, including sanding with wet sandpapers with the distribution of 240, 600, 800, and 1500 grit. After that, the specimen was polished with a combination of titanium (IV) oxide and ethanol. The specimen was etched using a nital 3%. Macrostructure observations were performed using a Dino-Lite digital microscope to investigate the weld penetration. Microstructure observations were carried out using an Olympus GX51 optical microscope to

determine the microstructure changes in each welding area. The tensile tests were performed using Tensilon RTF-2350 Universal Testing Machine with a maximum load of 50kN at a constant cross-head velocity of 5 mm/min. The specimens were prepared with a standard of ASTM E-8M. The fracture location of the tensile test results was observed using a scanning electron microscope (SEM) to observe the inside of the weld.

Table 3 - Welding parameters of the orbital pipe GTAW process [1]

No	Parameter code	Welding current (A)	Welding speed (mm/s)	Wire feeder speed (mm/s)
1	P-1509	150	0.9	
2	P-1510	150	1.0	
3	P-1511	150	1.1	
4	P-1609	160	0.9	
5	P-1610	160	1.0	1.4
6	P-1611	160	1.1	
7	P-1709	170	0.9	
8	P-1710	170	1.0	
9	P-1711	170	1.1	

3. Result and Discussion

3.1 Macrostructure

Macrostructure observations were carried out by making a cross-section of the welds at each welding position (0° , 90° , 180° , and 270°). The results of macrostructure observations at a welding current of 160 A and a welding speed of 1.0 mm/s can be seen in Figure 2. Figure 2a is at the welding position 0° , while Figure 2b is at the welding position 180° . The red line shows the original shape of the material before being welded, while the yellow line shows the boundaries of the weld area.

The welding position is 0° , the outside of the formed pipe tends to be flat or concave, while in the 180° position, the outside of the pipe that is formed tends to be convex. This is due to the influence of the gravitational force on orbital pipe welding [9]. In addition, at position 0° the weld penetration that occurs does not penetrate the inside of the pipe (shallow penetration), but at position 180° the weld penetration can penetrate to the inside of the pipe. This is because the initial position of the welding is at an angle of 330° , so when the welding reaches an angle of 0° , the heat is not enough to melt the material to the inside. However, when the welding begins to reach an angle of 90° to 360° , then the heat generated is enough or more to melt the material up to the inside of the pipe [10].

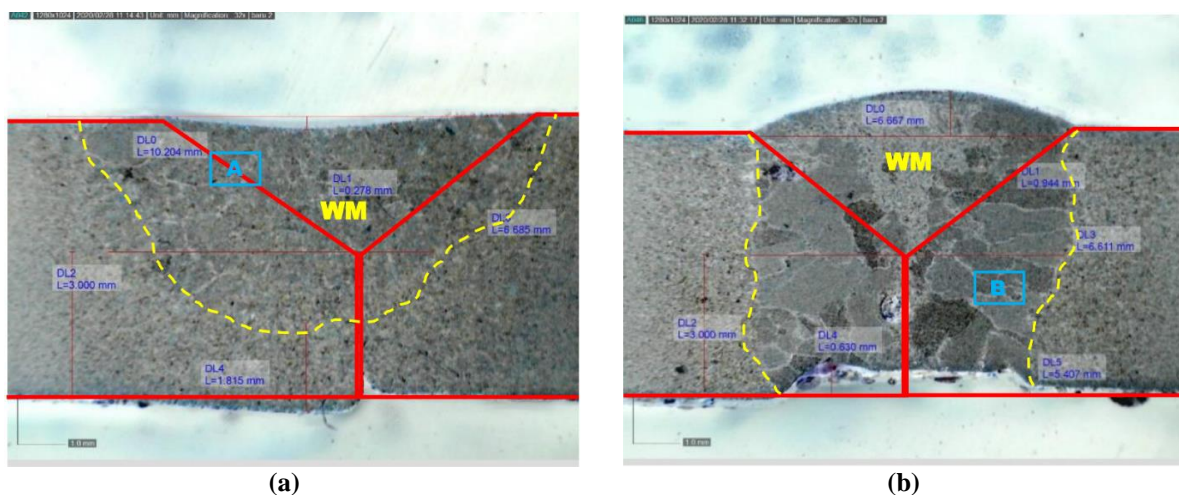
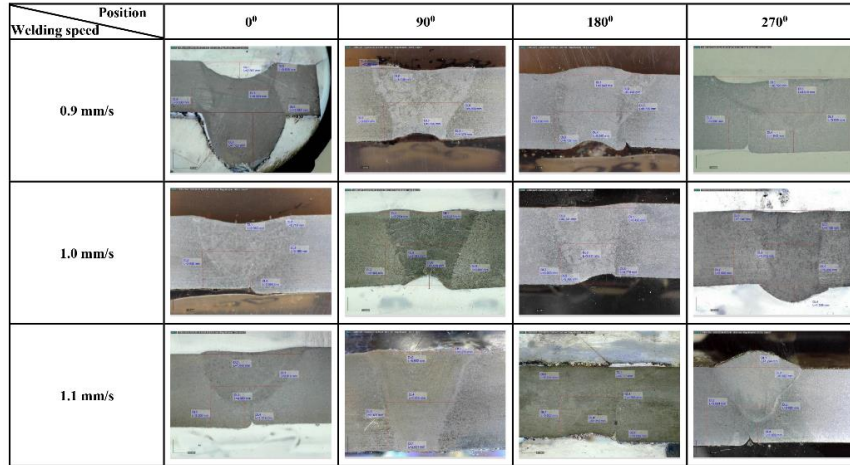


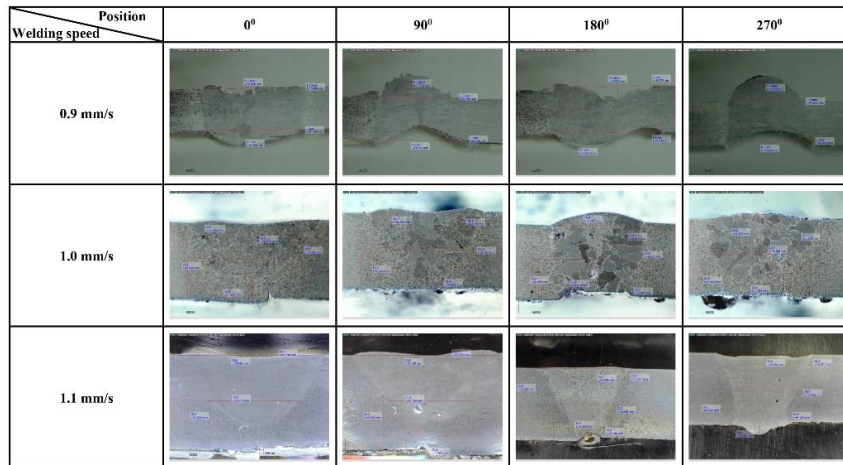
Fig. 2 - Macrostructure of A36 steel weld-on welding current 160 A, welding speed 1.0 mm/s and welding positions of (a) 0 degrees; (b) 180 degrees

Figure 3 shows the results of macrostructure observations at different welding speeds and welding positions. In addition, there are three variations of welding current: 150 A (Figure 3a), 160 A (Figure 3b), and 170 A (Figure 3c). Based on the results of macrostructure observations, it can be seen that increasing the welding speed will prevent weld

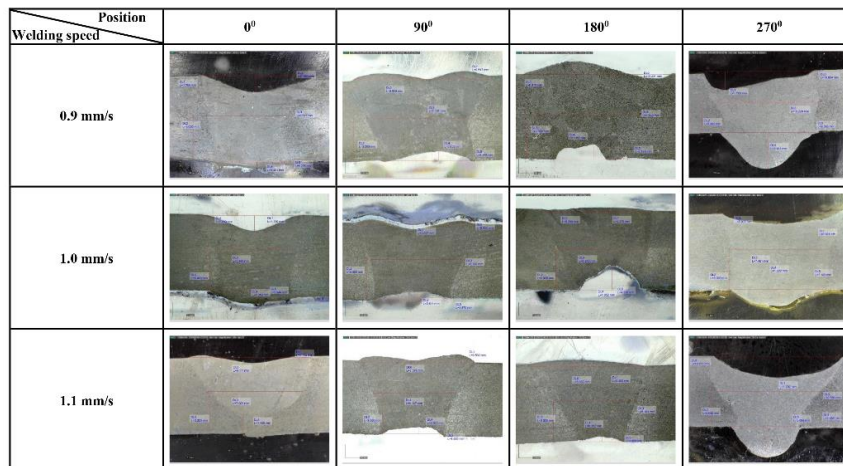
penetration at the welding position 0° and vice versa. Meanwhile, increasing the welding current can deepen the weld penetration in all welding positions. This is due to the different temperature changes that occur when varying welding speeds or welding currents [1]. Where if the welding speed is increased, the temperature at the start of welding up to position 0° is not high enough to melt the material to the inside. If the welding current is increased, the temperature at the start of the welding position up to position 0° can melt the material so that it gets inside and other welding positions, which will get deeper penetration.



(a)



(b)



(c)

Fig. 3 - Macrostructure of A36 steel weld on different welding speed and welding position with welding currents of (a) 150 A; (b) 160A; (c) 170 A

Another study by Singh et al. [11] proved that increasing the welding speed or welding current can increase thermal efficiency. This will directly affect the depth of weld penetration. The resulting penetration depth is from 2.9 mm to 5.3 mm. In general, increasing the welding current can increase the penetration depth, while increasing the welding speed, welding voltage and feed rate can decrease the penetration depth [12]. The depth of penetration in this study follows previous studies that several researchers have carried out. Welding current and welding speed influence the depth of penetration. Figueirôa et al. [9] reported that the weld position dramatically affects the weld geometry (bead width and penetration depth) formed in the weld. The force of gravity strongly influences weld positions 0° and 180° on the welding pips orbital while the weld positions 90° and 270° are not affected by gravity.

3.2 Microstructure

Microstructure observations were made on the weld metal (WM) area. Figure 4a shows the results of microstructural observations at a welding current of 160A, a welding speed of 1.0 mm/s, and a welding position of 0° . The welding area shown is in Figure 2a in the letter "A" in the box. Figure 4b shows the magnification of Figure 4a according to the red box. The results show that at position 0° , there are still a lot of ferrite structures, but little pearlite and martensite structures are formed. This is because, at position 0° , the temperature is not hot enough to change the base metal's microstructure, so the ferrite structure is still visible [5]. Figure 5a shows the results of microstructure observations at a welding current of 160A, a welding speed of 1.0 mm/s, and a welding position of 180° . The welding area shown is in accordance with Figure 2b in the letter "B" in the box. Figure 5b shows the magnification of Figure 5a according to the red box. The results of microstructure observations show that at the welding position of 180° , the structure formed was dominated by pearlite, martensite, and lath martensite. At the welding position 180° , the temperature reached is very high so that structural changes can occur homogeneously from the base metal [13].

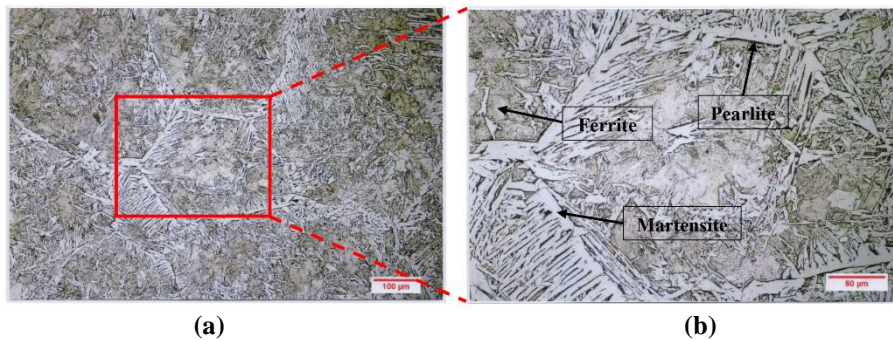


Fig. 4 - The microstructure of A36 steel weld-on welding current 160 A, welding speed 1.0 mm/s and welding position 0 degrees (a) 100 μm ; (b) 50 μm

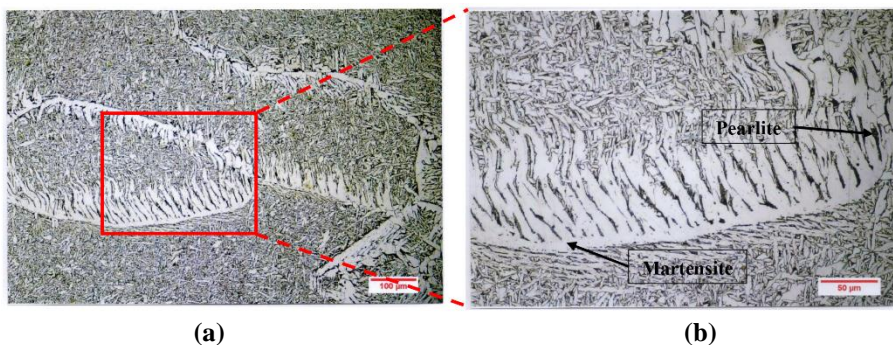


Fig. 5 - The microstructure of A36 steel weld-on welding current 160 A, welding speed 1.0 mm/s and welding position 180 degrees (a) 100 μm ; (b) 50 μm

Weld positions 0° and 180° have different temperature accumulations. At the 0° welding position, the temperature accumulation is still low because the welding starts at the 330° position and rotates clockwise, while at the 180° welding position, the temperature accumulation is higher. So that at 180° welding position has a coarser grain structure. Asibeluo et al. [14] reported that increasing the welding current can increase the grain structure roughness. The grain structure roughness is also dependent on the cooling rate during the welding process. The higher the cooling rate, the finer the structure formed. The degree of cooling in this welding depends on the heat input and working temperature.

3.3 Tensile Strength

The ultimate tensile strength (UTS) was plotted in different parameter codes and welding positions (Figure 6). Figure 6a, b, c, and d represents the UTS in welding positions of 0°, 90°, 180°, and 270°, respectively. The UTS for welding positions 0°, 180°, and 270° several parameters experience a decrease in tensile strength while at the 90° welding position almost all parameters, the tensile strength is above the base metal. A welding current of 170 A and a welding speed of 0.9 mm/s produce the highest UTS is 502.80 MPa, while a welding current of 150 A and a welding speed of 0.9 mm/s have the lowest UTS is 280.77 MPa. This shows an increase in tensile strength of 11.01% of the base metal and a decrease in tensile strength of 38.01% of the base metal.

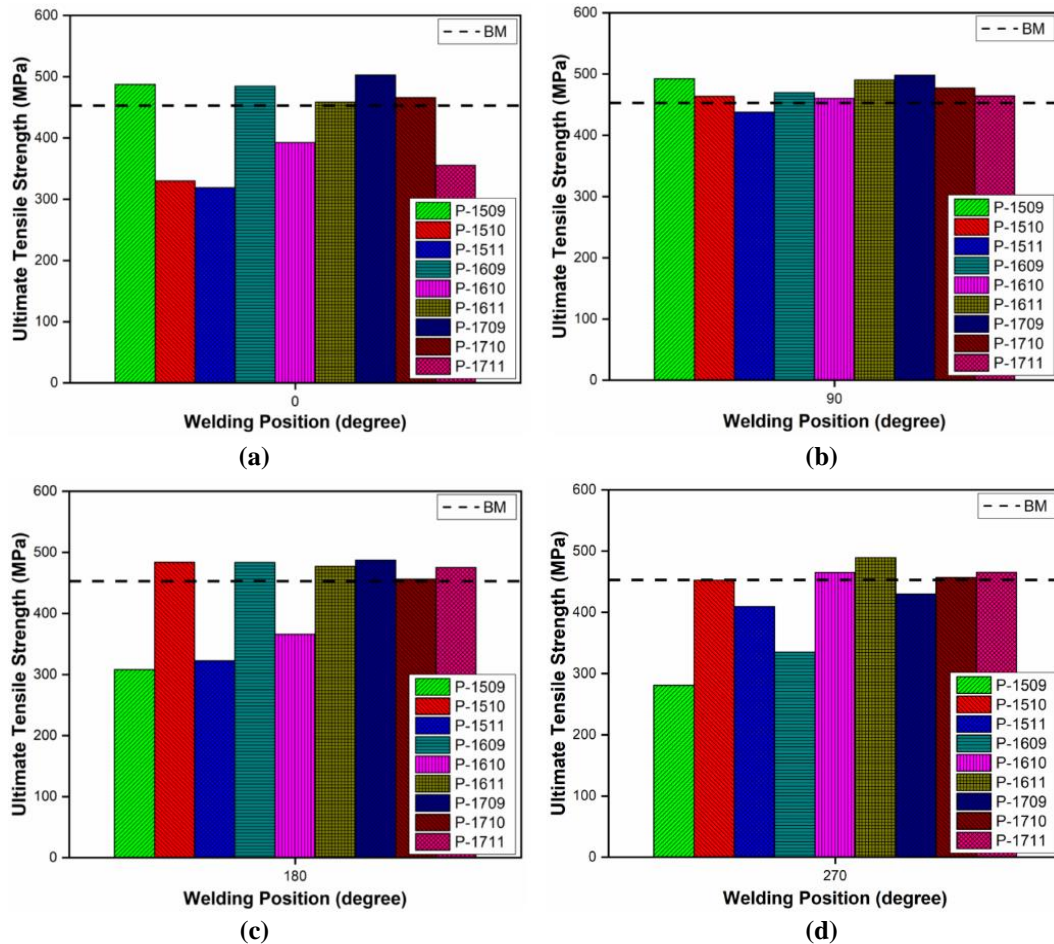


Fig. 6 - Ultimate tensile strength (UTS) in different parameters and welding positions of (a) 0°; (b) 90°; (c) 180°; (d) 270° in comparison to base metal (BM)

Heat input and temperature distribution received by the material have an influence on tensile strength [15, 16]. The welding position of 0°, the temperature distribution received by the material, is still relatively low, so that the mixture between added material and base metal is not homogeneous for several parameters. In contrast to the welding positions of 180° and 270°, the temperature distribution received by the material is sufficient or exceeds to make the mixture of added material and base metal homogeneous for several parameters. In another case, with the welding position of 90°, the temperature distribution at this welding position is very suitable to make the mixture between the added material and the base metal mixed homogeneously, so that the UTS produced at the 90° welding position is more stable than the other welding positions.

Increasing the welding current can increase the heat input as well as decrease the welding speed. With high heat input, the base metal and filler metal can melt well so that a homogeneous mixture occurs [17]. In addition, the penetration depth can be achieved well if the heat input is high. However, if the heat input is too high, welding defects can occur in the form of excessive penetration until the material is perforated. Welding position also influences the formation of weld penetration. This difference in welding position is due to the accumulation of temperature from the start of welding to the end of welding. The 0° welding position has a low-temperature accumulation, the 90° – 180° welding position has begun to increase the temperature accumulation, and at the 180° – 270° welding position, the temperature accumulation is very high until the welding ends. The amount of temperature accumulation will affect the depth of penetration at each welding position. This will directly affect the maximum tensile strength of the weld. Jha et

al. [17] reported the results of their research that the welding current of 120 A produced the highest maximum tensile strength. There is a decrease in the ultimate tensile strength at welding currents of 130 A and 140 A.

Welding positions at 0°, 180°, and 270°, several parameters experience a decrease in tensile strength, especially at a welding current of 150 A. The heat generated at a welding current of 150 A is the lowest among other parameters. At a welding position of 0°, the accumulated temperature is still too low. The mixture between the base metal and filler metal is less homogeneous, and there is a lack of weld penetration. At a welding position of 180°, the temperature accumulation is quite high, but because the pressure at the welding current of 150 A is less able to push the molten metal, which is affected by gravity so that in this position, there is less penetration. At a welding position of 270°, the temperature accumulation is very high, so that because there is no influence of gravity, excessive penetration occurs. Bermejo et al. [18] stated that there was no clear correlation between the position of the weld and its mechanical properties. Meanwhile, according to Figueirôa et al. [9] weld position has an influence on the microstructure and microhardness of the orbital pipe welding.

The fracture location of the tensile test results can be seen in Figure 7. There are two fracture locations, the first fracture occurred in the weld area shown in number 1 in Figure 7, and the second fracture happened in the base metal area shown in number 2 in Figure 7. The fracture in the weld area indicates that the UTS is lower or the same as the base metal because the mixture between the added material and the base metal is less homogeneous. The depth of the weld penetration is not deep. Meanwhile, the fracture in the base metal area shows that the UTS is above the base metal because the mixture between added material and base metal is relatively homogeneous. The depth of weld penetration is deep enough to the inside of the pipe. The location of the fracture that occurred in the weld area (number 1) then analyzed the fracture surface of the specimen using SEM, and the SEM image was shown in Figure 8. Figure 8a shows the fracture surface, and there was a micro-void. The high magnification image of the fracture surface was used to ensure the presence of fibrous and dimples (Figure 8b) due to this was related to the ductile of the material being observed, a similar thing was reported by Vinoth Kumar [19].

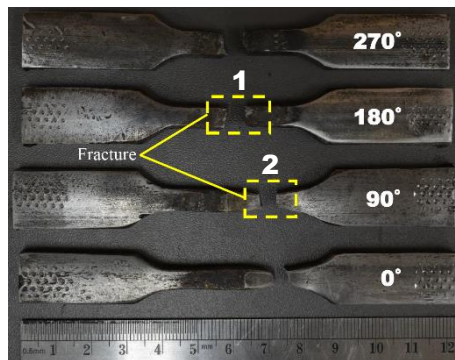


Fig. 7 - The fracture location of the tensile test results

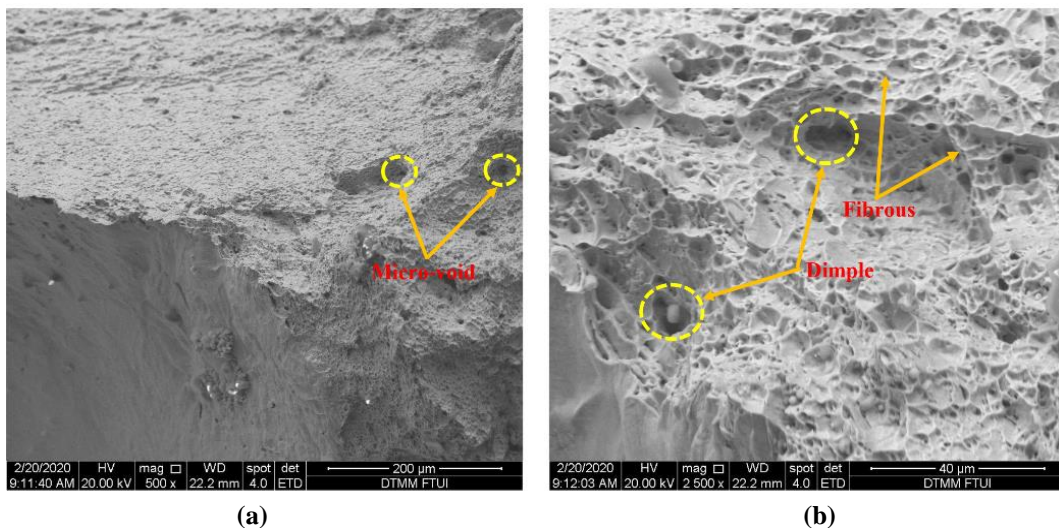


Fig. 8 - SEM image of a fracture surface of the tensile test (a) low magnification; (b) high magnification

4. Conclusions

In this work, the influence of the weld parameters on the GTAW orbital pipe welding was evaluated. The results of the macro-graphic analysis show that increasing the welding speed can lower the weld penetration depth, especially at the welding position 0°, while increasing the welding current can deepen the weld penetration depth at all welding positions. The results of the micro-graphic analysis show that at the welding position 0°, the microstructure is still dominated by ferrite with little pearlite and martensite structures, but at the welding position 180°, the microstructure has been dominated by pearlite, martensite, and lath martensite structures. The ultimate tensile strength (UTS) at the 90° welding position is more stable and above the base metal than other welding positions. The highest UTS increase occurred in the welding current parameter of 170 A, welding speed of 0.9 mm/s, and welding position 0° of 11.01% from the base metal. In comparison, the lowest decrease in UTS occurred in the welding current parameter of 150 A, welding speed of 0.9 mm/s, and welding position 270° of 38.01% from the base metal. The highest and lowest ultimate tensile strength is 502.80 MPa and 280.77 MPa, respectively. The results of the analysis of the fracture surface that occurred in the weld area showed that there were micro-voids and dimples in the welding area, which caused a decrease in tensile strength.

Acknowledgment

This work is supported by the Master Program to Doctorate for Scholar Excellent (PMDSU) program of the Ministry of Research & Technology and High Education (RISTEK DIKTI) 2020 with contract number NKB-437/UN2.RST/HKP.05.00/2020.

References

- [1] Panji, M., A.S. Baskoro, and A. Widianto. (2019). Effect of Welding Current and Welding Speed on Weld Geometry and Distortion in TIG Welding of A36 Mild Steel Pipe with V-Groove Joint. *IOP Publishing*
- [2] Lukkari, J. (2005). Orbital-TIG—a great way to join pipes. *The ESAB Welding and Cutting Journal*. **60**(01): p. 3-6
- [3] Aisc, A. (2005). Steel Construction Manual; American Institute of Steel Construction. *Inc.*—
- [4] Baskoro, A.S., R. Hidayat, A. Widianto, M.A. Amat, and D.U. Putra. (2019). Optimization of Gas Metal Arc Welding (GMAW) Parameters for Minimum Distortion of T Welded Joints of A36 Mild Steel by Taguchi Method. *Trans Tech Publ*
- [5] Feujofack Kemda, B.V., N. Barka, M. Jahazi, and D. Osmani (2019). Optimization of resistance spot welding process applied to A36 mild steel and hot dipped galvanized steel based on hardness and nugget geometry. *International Journal of Advanced Manufacturing Technology*
- [6] Liying, L., X. Jun, H. Bin, and W. Xiaolei (2020). Microstructure and mechanical properties of welded joints of L415/316L bimetal composite pipe using post internal-welding process. *International Journal of Pressure Vessels and Piping*. **179**: p. 104026
- [7] Fan, J.W., J. Luo, J.J. Gao, F.H. Bo, Q. Ren, H.X. Lin, and H.B. Geng (2020). Mechanical properties and microstructure of longitudinal submerged arc welded joint of a new C–Mn steel sheet cladding fine grained ferrite in surface layer for a long distance transport pipeline. *Materials Research Express*. **7**(4): p. 046513
- [8] Lawal, T.F., M.O.H. Amuda, F.S. Omonua, and K.S. Enumah (2020). Microstructure and Mechanical Properties in Thermally Treated Cr-Mn-Cu Stainless Steel Welds. *International Journal of Integrated Engineering*. **12**(4): p. 161-171
- [9] Figueirôa, D.W., I.O. Pigozzo, R.H.G.e. Silva, T.F.d.A. Santos, and S.L. Urtiga Filho (2017). Influence of welding position and parameters in orbital tig welding applied to low-carbon steel pipes. *Welding international*. **31**(8): p. 583-590
- [10] Kemda, B.V.F., N. Barka, M. Jahazi, and D. Osmani (2019). Modeling of phase transformation kinetics in resistance spot welding and investigation of effect of post weld heat treatment on weld microstructure. *Metals and Materials International*. p. 1-19
- [11] Singh, B., P. Singhal, and K.K. Saxena (2019). Investigation of Thermal Efficiency and Depth of Penetration during GTAW Process. *Materials Today: Proceedings*. **18**: p. 2962-2969
- [12] Singh, R.P. and M.K. Agrawal (2021). Influence of process parameters on depth of penetration of tungsten inert gas welded joints for low carbon steel AISI 1010 plates. *Materials Today: Proceedings*
- [13] Baskoro, A.S., M.A. Amat, A.I. Pratama, G. Kiswanto, and W. Winarto (2019). Effects of tungsten inert gas (TIG) welding parameters on macrostructure, microstructure, and mechanical properties of AA6063-T5 using the controlled intermittent wire feeding method. *The International Journal of Advanced Manufacturing Technology*. **105**(5-6): p. 2237-2251
- [14] Asibeluo, I.S. and E. Emifoniye (2015). Effect of arc welding current on the mechanical properties of A36 carbon steel weld joints. *SSRG International Journal of Mechanical Engineering*. **2**(9): p. 32-40

- [15] Karunakaran, N. (2012). Effect of pulsed current on temperature distribution, weld bead profiles and characteristics of GTA welded stainless steel joints. *International Journal of Engineering and Technology*. **2**(12)
- [16] Kulkarni, S., P.K. Ghosh, and S. Ray (2008). Improvement of weld characteristics by variation in welding processes and parameters in joining of thick wall 304LN stainless steel pipe. *ISIJ international*. **48**(11): p. 1560-1569
- [17] Jha, R. and A.K. Jha (2014). Investigating the Effect of Welding Current on the Tensile Properties of SMAW Welded Mild Steel Joints. *International Journal of Engineering Research*. **3**(4)
- [18] Bermejo, M.A.V., L. Karlsson, L.-E. Svensson, K. Hurtig, H. Rasmuson, M. Frodigh, and P. Bengtsson (2015). Effect of welding position on properties of duplex and superduplex stainless steel circumferential welds. *Welding in the World*. **59**(5): p. 693-703
- [19] Kumar, M.V. and V. Balasubramanian (2014). Microstructure and tensile properties of friction welded SUS 304HCu austenitic stainless steel tubes. *International Journal of Pressure Vessels and Piping*. **113**: p. 25-31